JOURNAL OF THERMOPHYSICS AND HEAT TRANSFER
Vol. 20, No. 1, January–March 2006

Temperature and Wavelength-Dependent Spectral Absorptivities of Metallic Materials in the Infrared

Samuel B. Boyden*
New Mexico State University, Las Cruces, New Mexico 88003
and
Yuwen Zhang†
University of Missouri-Columbia, Columbia, Missouri 65211

The optical constants and absorptivity of selected elemental metals and alloys are calculated based on the Drude-type model. The calculations are made primarily at the CO_2 (10.6-μm) and the Nd:YAG (1.06-μm) laser wavelengths, with consideration for laser material processing. The absorptivities at these wavelengths are calculated for some important metallic materials. For the application of laser material processing, temperature-dependent values are calculated based on available experimental data. The absorptivity values for alloys are calculated by assuming that the sum of contributions of the proportionality of the valence electrons to the effective mass of an electron for each constituent metal is equal to the proportionality of the valence electrons to the effective mass of an electron for the alloy. The absorptivities of the elemental metals at 10.6 μm agreed with experimental data very well, except for transition metals. Agreement of alloy and element absorptivity calculated values and experimental data is good at 10.6 μm but not at 1.06 μm. Overall the calculation by the Drude model gives good estimates of absorptivity at 10.6 μm.

Nomenclature

e = electron electric charge, C
k = complex refractive index, dimensionless
m = mass of the electron, kg
m^* = optical mass of the electron, kg
N = number of free electrons per cubic centimeter
n = refractive index, dimensionless
R = reflectivity, dimensionless
T = temperature, K
α = spectral absorptivity, dimensionless
γ = damping frequency, s^{-1}
ε_0 = permittivity of free space, $F \cdot m^{-1}$
λ = wavelength of incident radiation, μm
ρ = resistivity of material, ohm $\cdot$ m
σ_0 = conductivity of material, $ohm^{-1} \cdot m^{-1}$
τ = relaxation time of electrons, s
ω = angular frequency of radiation, $rad \cdot s^{-1}$
ω_P = plasma frequency, $rad \cdot s^1$

Introduction

ANY model for laser processing of materials must have a complete description of the coupling between the laser source and the material. The coupling is defined by the spectral absorptivity of the material at the wavelength of operation; hence, the normal spectral absorptivity is a critical parameter of interest for many applications in this area.[1] Optical properties of bulk metals are typically functions of wavelength, temperature, surface geometry (roughness), incident intensity, and physical atomic structural and electrical properties of the material. Because absorptivity is dependent on temperature, it is also important to consider the absorptivity change in the modeling of laser heating.[2]

Wavelength-dependent absorptivity data may be found by Touloukian,[3] Touloukian and DeWitt,[4] and Touloukian and Ho.[5] Temperature-dependent absorptivity data are few,[6] possibly due to the difficulty in conducting temperature-dependent experiments. The experimental study by Wieting and Schriempf[7] provides the only temperature-dependence absorptivity data available for alloys. Zhang and Modest[8] presented experimental results on temperature-dependent absorptances of ceramics for Nd:YAG and CO_2 laser processing applications. Temperature-dependent absorptivity of many metallic materials at the temperature near their melting points is not directly available in the existing literature.

Although obtaining the absorptivity value from experimental investigation is preferred, calculation of the absorptivity based on a theoretical model is also important for the situation when the absorptivity is not readily available for a particular material of interest. One method to predict the absorptivity of an electromagnetic field that obeys Maxwell's equations is to use the following equation based on the Fresnel reflection relation:

$$\alpha = 1 - R = 1 - \frac{(n-1)^2 + k^2}{(n+1)^2 + k^2} \tag{1}$$

where n and k are the real and imaginary parts of refractive index, which can be determined using various models. The Drude theory is a modified oscillator-type model developed for reflection and absorption estimation and has been used by many researchers (see Refs. 9–12). This model uses the electrical properties of the material and optical properties of the material. The Hagen–Ruben relation is a model, which provides ease of calculation and can be applied for frequencies much less than the mean collision rate of the electrons in the metal.[13] Sokolov[14] presented a method of determining optical properties of alloys, with a modified damping function. Dausinger and Shen[6] provided temperature-dependent models based on the Drude model. Weaver and Frederikse[15] presented a compilation of data sets for a number of practical metals.

The temperature-dependent absorptivity of selected pure metals and alloys at infrared regions of the electromagnetic spectrum were calculated and will be presented and compared with the existing experimental data. The absorptivity values of the selected metals are of necessity for accurate laser processing models.

Received 11 January 2005; revision received 28 April 2005; accepted for publication 28 April 2005.

*Graduate Research Assistant, Department of Mechanical Engineering.
†Associate Professor, Department of Mechanical and Aerospace Engineering. Senior Member AIAA.

Predictive Methods

Drude Theory

Prediction of absorptivity using Eq. (1) requires knowledge of the real and imaginary parts of the refractive index. One widely used model is Drude theory, which predicts the absorptivity of conducting materials in the infrared and visible wavelengths using a free electron model (see Refs. 9–12). The equations of the Drude theory are expressed as

$$n^2 - k^2 = 1 - \omega_p^2(\omega + \tau^{-2}) \tag{2}$$

$$2nk = \omega_p^2 \big/ [\omega\tau(\omega^2 + \tau^{-2})] \tag{3}$$

When both n and k are real and positive, Eqs. (2) and (3) can be solved to yield[10]

$$n = \left(1\big/\sqrt{2}\right)\left\{[(1-Q)^2 + (Q/\omega\tau)^2]^{\frac{1}{2}} - Q + 1\right\}^{\frac{1}{2}} \tag{4}$$

$$k = \left(1\big/\sqrt{2}\right)\left\{[(1-Q)^2 + (Q/\omega\tau)^2]^{\frac{1}{2}} + Q - 1\right\}^{\frac{1}{2}} \tag{5}$$

where

$$Q = \omega_p^2 \big/ (\omega^2 + \tau^{-2}) \tag{6}$$

The plasma frequency can be expressed as[10]

$$\omega_p^2 = \left(Ne^2 \big/ m^* \varepsilon_0\right)^{\frac{1}{2}} \tag{7}$$

and the relaxation time, or electron lifetime, is

$$\tau = \left(m^* \sigma_0 \big/ Ne^2\right) \tag{8}$$

Damping frequency is inversely related to relaxation time, that is,

$$\gamma = 1/\tau \tag{9}$$

Alloys

The absorptivities for alloys will also be calculated using Drude theory. It is assumed that each constituent metal is contributing the total free electrons according to its concentration in the alloy, so that parameters N/m^* and γ for the alloys can be approximated by summing the contributions of each group, even though these alloys have complex Fermi surfaces and substantial structure disorder.[7] In addition, the absorptivities of alloy are not sensitive to N/m^*, and the ratio can be approximated[7] by assuming $m^* = m$. For the case when an optical electron mass was available, this was used in the calculation, otherwise the free electron mass was used, as in the case with aluminum ($m^* = 1.32 \times 10^{-30}$ kg).

The accuracy of the predicted absorptivity depends on the accuracy of the optical constants, which are obtained experimentally by different researchers. In addition, surface roughness, contamination, and oxidization can also be the source of errors, especially for high-temperature laser material processing. Because this model does not take into account surface roughness, the material surface should be smooth and the materials under consideration should be nominally pure to get results that reasonably agree with the experiments. When experimental absorptivity and reflectivity data are selected, care was taken in selecting polished materials without oxidation or sandblasting. Whereas the accuracy of these optical constants varies, the most reliable way to validate the predicted the absorptivity is to compare it with the available experimental data. The absorptivity of the pure metal and alloys will be predicted and compared with the experimental data in the next section.

Results and Discussion

Absorptivities of Pure Metals

Ordal et al.[9] collected optical constants data from the literature, and calculated the Drude parameters ω_p and γ for six metals to see if the experimental data fit to the Drude model. Their results show that the transition metals did not fit with the Drude model, except tungsten, and that noble metals fit well. Arnold[10] obtained absorptivities of Ag, Au, Al, Cu, Pb, and W at 10.6 μm using optical data by Ordal et al.[9] and Drude theory. The predicted absorptivities of Ag, Au, Al, and Cu at room temperature were compared with the available experimental data but no comparison was made at elevated temperature. Based on Arnold's method,[10] the Drude parameters and optical constants were calculated using Eqs. (2) and (3), then the temperature-dependent absorptivities were computed for three metals, Al, Cu, and Ni, using temperature-dependent conductivity data. The results are summarized in Tables 1–3, respectively. The conductivity values in Tables 1–3 that were used in calculating Drude parameters were calculated from the resistivity values obtained from Lide.[16] These calculated absorptivity values were plotted with experimental data[4] in Figs. 1–3. Selection of experimental data with similar sample preparation and nominal composition was intended for consistency. Surface conditions of the sample material experimental were selected with either as received unmodified or as polished and without oxidation or sandblasting, as described.[4] The lines of the least-square fit for the calculations in Figs. 1 and 2 were given by Arnold.[10] Because of the scarcity of temperature-dependent absorptivity data in the literature, only a few experimental data were plotted for comparison (Figs. 1–3). Also note, as seen in

Table 1 Calculated absorptivity at 10.6 μm for aluminum

Temperature, K	Conductivity $\sigma \times 10^7$, mho · m^{-1}	Resistivity $\rho \times 10^{-8}$, ohm · m	Plasma frequency $\omega_p \times 10^{16}$, rad/s	Relaxation time $\tau \times 10^{-14}$, s	n	k	Reflectivity	Absorptivity
300	3.660	2.733	1.992	1.040	25.700	101.665	0.991	0.009
400	2.580	3.87	1.992	0.734	31.938	94.380	0.987	0.013
500	2.000	4.99	1.992	0.569	35.785	87.288	0.984	0.016
600	1.630	6.13	1.992	0.464	38.014	80.700	0.981	0.019
700	1.360	7.35	1.992	0.387	39.164	74.532	0.978	0.022
800	1.150	8.70	1.992	0.327	39.524	68.726	0.975	0.025
900	0.982	10.18	1.992	0.279	39.289	63.413	0.972	0.028

Table 2 Calculated absorptivity at 10.6 μm for copper

Temperature, K	Conductivity $\sigma \times 10^7$, mho · m^{-1}	Resistivity $\rho \times 10^{-8}$, ohm · m	Plasma frequency $\omega_p \times 10^{16}$, rad/s	Relaxation time $\tau \times 10^{-14}$, s	n	k	Reflectivity	Absorptivity
300	5.797	1.725	1.636	2.448	10.096	89.619	0.995	0.005
400	4.163	2.402	1.636	1.758	13.663	88.114	0.993	0.007
500	3.236	3.090	1.636	1.366	16.944	86.228	0.991	0.009
600	2.637	3.792	1.636	1.113	19.895	84.031	0.989	0.011
700	2.215	4.514	1.636	0.935	22.507	81.586	0.988	0.012
800	1.900	5.262	1.636	0.802	24.775	78.952	0.986	0.014
900	1.655	6.041	1.636	0.699	26.704	76.186	0.984	0.016

Table 3 Calculated absorptivity at 10.6 μm for nickel

Temperature, K	Conductivity $\sigma \times 10^7$, mho · m^{-1}	Resistivity $\rho \times 10^{-8}$, ohm · m	Plasma frequency $\omega_p \times 10^{16}$, rad/s	Relaxation time $\tau \times 10^{-14}$, s	n	k	Reflectivity	Absorptivity
300	1.390	7.200	0.322	15.120	0.008	2.444	0.996	0.004
400	0.847	11.800	0.322	9.223	0.013	2.444	0.993	0.007
500	0.565	17.700	0.322	6.149	0.019	2.444	0.989	0.011
600	0.392	25.500	0.322	4.268	0.027	2.444	0.984	0.016
700	0.312	32.100	0.322	3.390	0.034	2.443	0.980	0.020
800	0.282	35.500	0.322	3.066	0.038	2.443	0.978	0.022
900	0.259	38.600	0.322	2.819	0.041	2.443	0.976	0.024

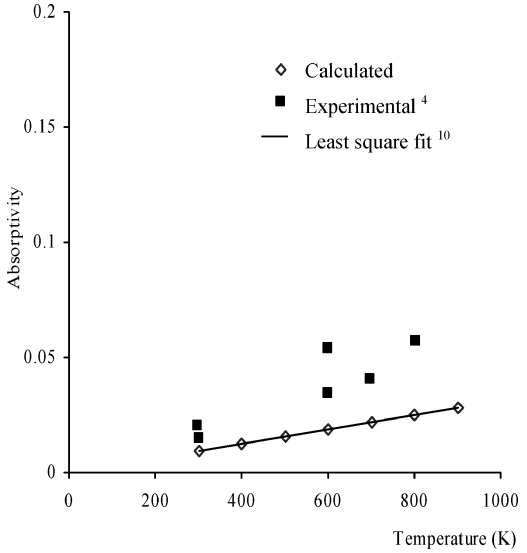

Fig. 1 Temperature-dependent absorptivity for aluminum (10.6 μm).

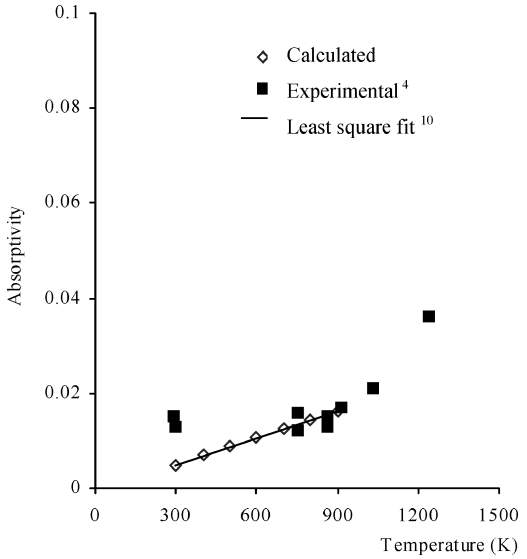

Fig. 2 Temperature-dependent absorptivity for copper (10.6 μm).

Figs. 1–3 there is inconsistency among the experimental data. This is probably because the experimental data for the pure metals were from different researchers and placed together, which would naturally produce some inconsistency among the results. The maximum deviation determined by a linear extrapolation of the temperature-dependent experimental values for the pure metals considered did not exceed 5%; 3.61% for aluminum, 1.22% for copper, and 3.58% for nickel. These error estimates for pure metals are in agreement with the room-temperature calculation obtained by Dausinger and Shen[6] for iron at wavelengths 0.5–15 μm.

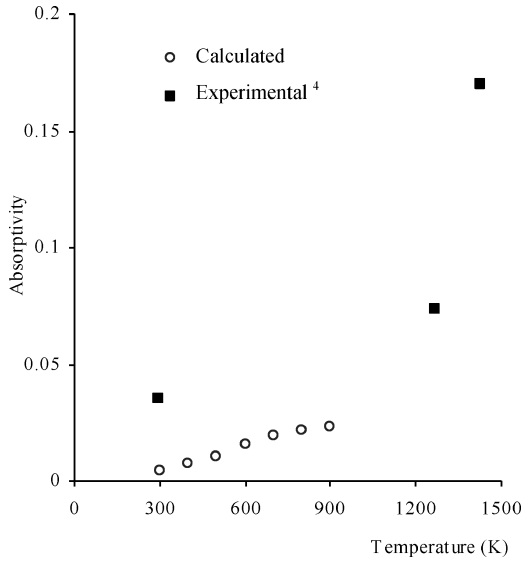

Fig. 3 Temperature-dependent absorptivity for nickel (10.6 μm).

Note from Figs. 1–3 that the calculated absorptivities are lower than the experimental values. Because surface roughness significantly influences the absorptivity values,[6,7] this could account for the higher absorptivity values in the experimental data. Considerable deviation is observed in the nickel data as shown in Fig. 3. Transition metals are known for the deviation from the Drude model because the interband absorption takes place even at lower energy. (see Ref. 6). Noble metals, on the other hand, are known to fit the Drude model better than the transition metals (see Ref. 6). Therefore, the deviation in nickel absorptivity values from the calculated values could be caused by the interband contribution.

Absorptivities of Alloys

We calculated the absorptivity of AISI 304 stainless steel over a range of wavelengths and temperatures and tabulated and plotted the results in Tables 4 and 5 and Figs. 4 and 5. Also, in Fig. 4 are the experimental results from Touloukian and DeWitt[4] and Wieting and Schriempf.[7] The experimental data were selected the same as described for the pure metals. The calculated absorptivity of the major component in AISI 304, Fe, is also shown in Fig. 4. The absorptivity of AISI 304 is higher than that of pure iron metal, which is in agreement with Dausinger and Shen.[6] The temperature-dependent absorptivity of AISI 304 at 10.6 μm is also calculated, and the results are given in Table 5 and Fig. 5. Near 1.06 μm, a peak in absorptivity is present in the experimental data; this indicates a wavelength at which efficient processing can be obtained. Theoretical values of AISI 304 were calculated based on the resistivity for high alloy steel En 58A302S25 (composition of 0.08% C, 0.3–0.5%Mn, 8% Ni, 18–20% Cr, and the balance Fe), because temperature-dependent resistivity data for AISI 304 (0.08% C, 19% Cr, 2% Mn, 10% Ni, and 1% Si) were not available. The experimental results from Wieting and Schriempf[7] are also plotted in Fig. 5 for comparison. It can be seen from Figs. 4 and 5 that our calculated results agreed very well

Table 4 Calculation of wavelength-dependent Drude parameters and optical constants for AISI 304

$N/m^* \times 10^{59}$, $kg^{-1} \cdot m^{-1}$	Resistivity $\Omega \times 10^{-7}$, ohm · m	Conductivity $\sigma \times 10^6$, ohm · m^{-1}	Plasma frequency $(Ne^2/m^*\varepsilon_0)$, $\omega_p \times 10^{16}$	Relaxation time $(m^*\sigma_0/Ne^2)$ $\tau \times 10^{-16}$	Wavelength λ, μm	n	k	Reflectivity	Absorptivity
1.771	7.200	1.389	2.266	3.056	0.100	0.184	0.662	0.599	0.401
1.771	7.200	1.389	2.266	3.056	0.500	1.863	4.804	0.762	0.238
1.771	7.200	1.389	2.266	3.056	1.000	4.281	7.303	0.789	0.211
1.771	7.200	1.389	2.266	3.056	2.000	7.632	10.075	0.827	0.173
1.771	7.200	1.389	2.266	3.056	3.000	9.997	12.049	0.850	0.150
1.771	7.200	1.389	2.266	3.056	4.000	11.907	13.702	0.866	0.134
1.771	7.200	1.389	2.266	3.056	5.000	13.549	15.162	0.877	0.123
1.771	7.200	1.389	2.266	3.056	6.000	15.012	16.488	0.886	0.114
1.771	7.200	1.389	2.266	3.056	7.000	16.343	17.712	0.894	0.106
1.771	7.200	1.389	2.266	3.056	8.000	17.573	18.855	0.900	0.100
1.771	7.200	1.389	2.266	3.056	9.000	18.722	19.931	0.905	0.095
1.771	7.200	1.389	2.266	3.056	10.000	19.804	20.952	0.909	0.091
1.771	7.200	1.389	2.266	3.056	11.000	20.830	21.925	0.913	0.087
1.771	7.200	1.389	2.266	3.056	12.000	21.807	22.856	0.916	0.084

Table 5 Calculation of temperature-dependent Drude parameters and optical constants for AISI 304 at 10.6 μm

Temperature, K	$N/m^* \times 10^{59}$, $kg^{-1} \cdot m^{-1}$	Resistivity $\Omega \times 10^{-7}$, ohm · m	Conductivity $\sigma \times 10^6$, ohm · m^{-1}	Plasma frequency $(Ne^2/m^*\varepsilon_0)^{1/2}$, $\omega_p \times 10^{16}$	Relaxation time $(m^*\sigma_0/Ne^2)$, $\tau \times 10^{-16}$	n	k	Reflectivity	Absorptivity
298	1.771	7.200	1.389	2.266	3.056	20.349	21.468	0.911	0.089
373	1.771	7.760	1.289	2.266	2.836	19.645	20.642	0.908	0.092
473	1.771	8.500	1.176	2.266	2.589	18.817	19.682	0.904	0.096
673	1.771	9.760	1.025	2.266	2.254	17.619	18.316	0.897	0.103
873	1.771	10.720	0.933	2.266	2.053	16.846	17.446	0.892	0.108
1073	1.771	11.410	0.876	2.266	1.928	16.349	16.892	0.888	0.112
1273	1.771	11.960	0.836	2.266	1.840	15.983	16.486	0.886	0.114

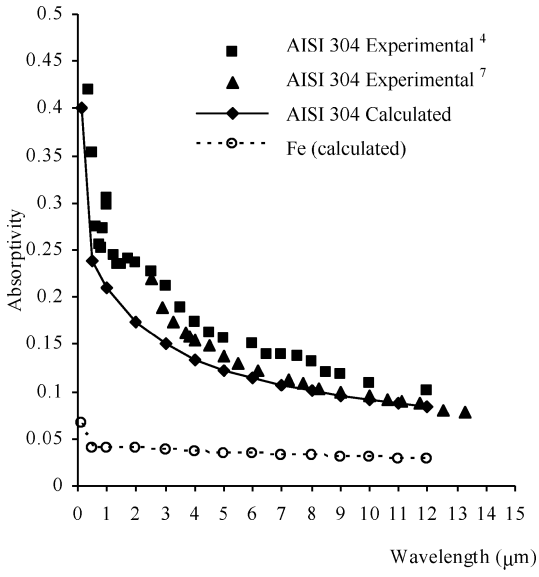

Fig. 4 Wavelength-dependent absorptivity for AISI 304 stainless steel (298 K).

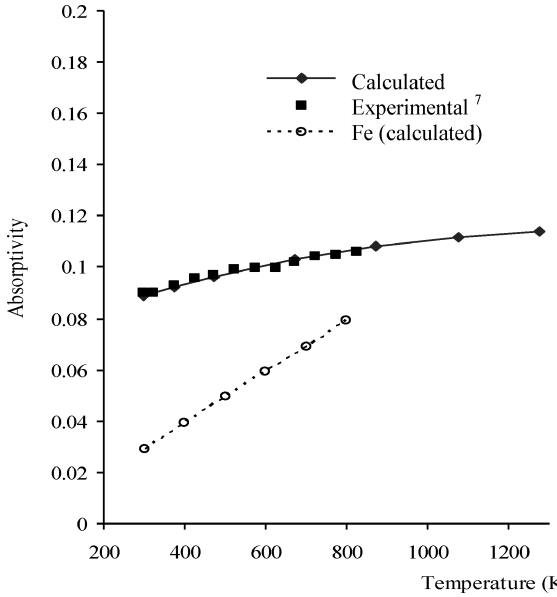

Fig. 5 Temperature-dependent absorptivity for AISI 304 (10.6 μm).

with the experimental data. It also can be seen that the absorptivity of alloys increases slowly with increase in temperature, which was the direct result of the conductivity in alloys varying diminutively with temperature.[7]

The method of calculating the absorptivity for Tables 4–7 uses temperature-dependent resistivity data of the alloy[3] and elemental properties of the constituents. With Eq. (7), the plasma frequency of the metal can be determined. For the alloys shown in Tables 4–7, the summation of the N/m^* ratio is used as the N/m^* value for the alloy. Temperature-dependent resistivity data were used to calculate the damping frequency using Eq. (8) as a function of temperature. These values were used in a straightforward manner for calculation of the complex refractive index, using Eqs. (4–6), from which the reflectivity can be determined with the Fresnel reflection relation. For Inconel (Table 6), the mass of an electron was used as m^* for the calculation except for Ni, where the proper effective mass was used. Also, the calculated results are based on temperature-dependent resistivity data for Inconel with a small amount of carbon (composition of 79.5 Ni, 13.0 Cr, 6.5 Fe, and 0.08 C). In Table 7, the electron mass was used to estimate m^* values, except for Al, Cu, Ni, and Zn. For Al 7075, the small component, that is, Cr = 0.3% was omitted in the calculation.

Table 6 Calculated temperature-dependent Drude parameters and optical constants of Inconel at 10.6 and 1.06 μm

Elements	Elemental $N/m^* \times 10^{59}$,[a] $\mathrm{kg}^{-1} \cdot \mathrm{m}^{-3}$	Fractional contribution $N/m^* \times 10^{59}$, $\mathrm{kg}^{-1} \cdot \mathrm{m}^{-3}$	Resistivity $\Omega \times 10^{-7}$, ohm · m	Conductivity $\sigma \times 10^{6}$, $\mathrm{mho} \cdot \mathrm{m}^{-1}$,	Relaxation time $(m^*\sigma_0/Ne^2)$, $\tau \times 10^{-16}$	n	k	Reflectivity	Absorptivity
Ni	1.003	0.797							
Cr	1.828	0.238							
Fe	1.864	0.121							
C	2.147	0.002							
Estimated values at 10.6 μm									
Temp (K)									
390.000		1.158	9.850	1.015	3.417	17.339	18.403	0.897	0.103
573.200		1.158	10.000	1.000	3.366	17.218	18.257	0.896	0.104
774.100		1.158	10.100	0.990	3.333	17.138	18.162	0.896	0.104
872.000		1.158	10.150	0.985	3.316	17.099	18.114	0.896	0.104
Estimated values at 1.06 μm									
Temp (K)									
390.000		1.158	9.850	1.015	3.417	3.526	6.279	0.765	0.235
573.200		1.158	10.000	1.000	3.366	3.529	6.233	0.762	0.238
774.100		1.158	10.100	0.990	3.333	3.531	6.202	0.761	0.239
872.000		1.158	10.150	0.985	3.316	3.532	6.187	0.760	0.240

[a]Mass of an electron was used for the calculation except for Ni.

Table 7 Calculation of Drude parameters and optical constants at room temperature for selected alloys at 10.6 μm

Elements	Elemental $N/m^* \times 10^{59}$, $\mathrm{kg}^{-1} \cdot \mathrm{m}^{-1}$	Fractional contribution $N/m^* \times 10^{59}$, $\mathrm{kg}^{-1} \cdot \mathrm{m}^{-1}$	Resistivity $\Omega \times 10^{-8}$, ohm · m	Conductivity $\sigma \times 10^{7}$, $\mathrm{mho} \cdot \mathrm{m}^{-1}$	Plasma frequency $(Ne^2/m^*\varepsilon_0)^{1/2}$, $\omega_p \times 10^{16}$	Relaxation time $(m^*\sigma_0/Ne^2)$, $\tau \times 10^{-16}$	n	k	Reflectivity	Absorptivity
Ti B120 VAC (Ti–V–Cr–Al)										
Ti	1.254	0.915								
V	1.586	0.206								
Cr	1.828	0.201								
Al	1.368	0.041								
Estimated values at 10.6 μm		1.364	149.000	0.067	1.988	1.918	14.312	14.777	0.874	0.126
Estimated values at 1.06 μm		1.364	149.000	0.067	1.988	1.918	3.632	5.010	0.688	0.312
A-110-AT (Ti-Al-Sn)										
Ti	1.254	1.160								
Al	1.368	0.068								
Sn	0.640	0.016								
Estimated values at 10.6 μm		1.244	163.000	0.061	1.899	1.921	13.685	14.127	0.868	0.132
Estimated values at 1.06 μm		1.244	163.000	0.061	1.899	1.921	3.475	4.785	0.676	0.324
Al 2024										
Al	1.368	1.278								
Cu	0.923	0.042								
Mg	0.945	0.014								
Mn	0.881	0.005								
Estimated values at 10.6 μm		1.339	5.330	1.876	1.970	54.605	35.697	84.799	0.983	0.017
Estimated values at 1.06 μm		1.339	5.330	1.876	1.970	54.605	0.526	10.562	0.982	0.018
Al 7075										
Al	1.368	1.238								
Zn	1.697	0.093								
Mg	0.945	0.024								
Cu	0.923	0.014								
Estimated values at 10.6 μm		1.3689	5.38	1.8587	1.9920	52.9066	36.4720	84.7617	0.9830	0.0170
Estimated values at 1.06 μm		1.3689	5.38	1.8587	1.9920	52.9066	0.5489	10.6790	0.9811	0.0189

The calculated results are also compared with experimental data in Figs. 6–10. Figure 6 shows Inconel absorptivity vs temperature, and it is seen that the calculated data have little variation due to the nearly constant resistivity values. Experimental data for Inconel at the wavelengths of interest were difficult to find; however, a few temperature-dependent points, reported experimental error[3] of 8.0%, show that a reasonable approximation was found by the Drude model. Figure 7 shows a good estimate for A-110-AT at 10.6 μm; however, at 1.06 μm the variation in experimental values used does not give a consistent picture for prediction at this wavelength for the model. For Fig. 8, at 10.6 μm the prediction by Drude theory is good, and there were no experimental values to compare at 1.06 μm. In Figs. 9 and 10 experimental and calculated data match well at 10.6 μm; however, at 1.06 μm a greater deviation from experiment is found. For the alloys considered, at 10.6 μm, the deviation from temperature-dependent experimental absorptivity did not exceed 6.0%: 0.56% for AISI 304, 5.18% for Inconel, and the deviation from the 10.6-μm room-temperature experimental values did not exceed 3.0% (1.36%) for Ti B120 VAC, 2.18% A-110-AT, 1.02% A1 2024, and 1% A1 7075. For Figs. 7–10, the agreement between calculated values and experimental data is good at 10.6 μm, but experimental values are much larger than those expected from the theory at 1.06 μm in all of the results. The higher absorption can be contributed by parallel band absorption, as shown by Ashcroft and Sturm.[17] This band does not appear in the Drude absorption theory. As shown in the case of aluminum, the parallel-band absorption occurs at a higher energy than the Drude theory predicts.

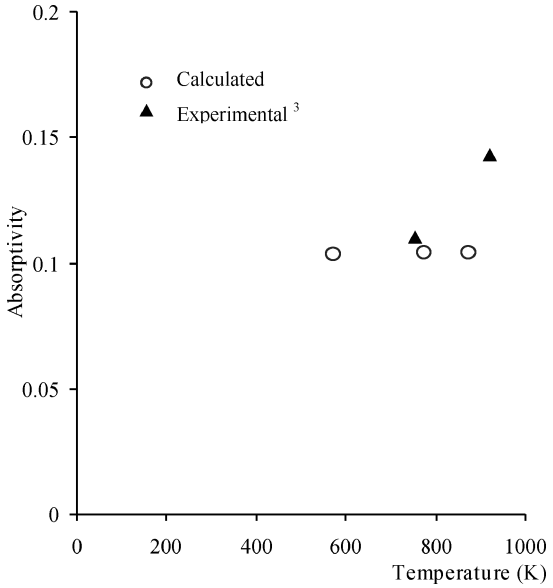

Fig. 6 Temperature dependent absorptivity for Inconel (10.6 μm).

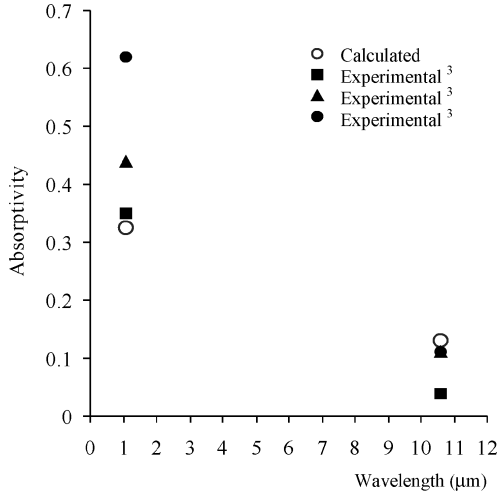

Fig. 7 Wavelength-dependent absorptivity for A-110-AT (298 K).

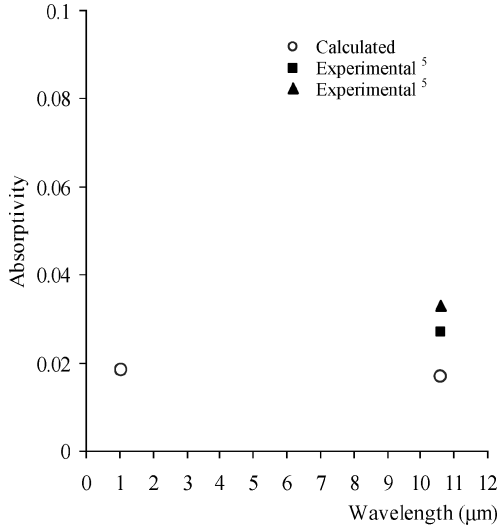

Fig. 8 Wavelength-dependent absorptivity for Al 2024 (298 K).

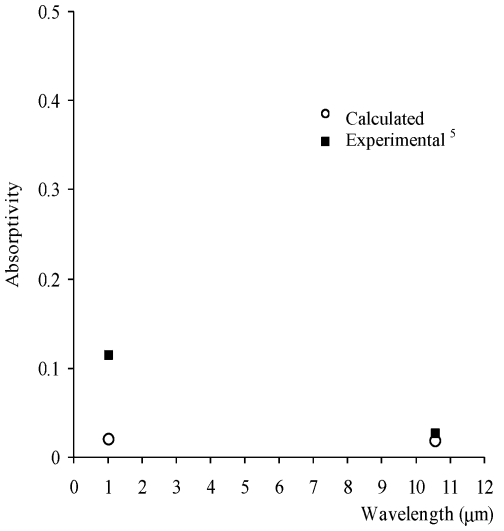

Fig. 9 Wavelength-dependent absorptivity for Al 7075 (298 K).

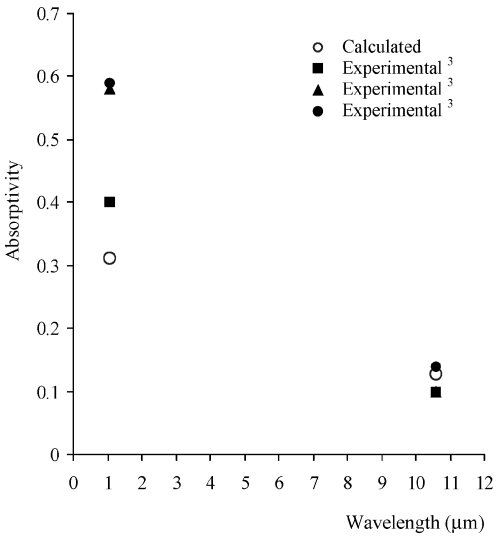

Fig. 10 Wavelength-dependent absorptivity for Ti B120 VAC (298 K).

Conclusions

The absorptivities of several selected pure metals and alloys were predicted using Drude theory. The predicted absorptivities of the pure metals at 10.6 μm agreed very well with the experimental results except for the transition metals due to interband absorption. Agreement of alloy and element absorptivity calculated values and the experimental data is good at 10.6 μm but not at 1.06 μm. The higher absorption at 1.06 μm can be attributed to parallel band absorption, which is not included in the Drude absorption theory. For practical purposes, this method provides a straightforward method of obtaining absorptivity values for metallic materials and generally works well for alloys at 10.6 μm. However, careful selection was required in trying to obtain experimental data with similar sample preparation and nominal composition for comparison with the calculated results to agree well.

Acknowledgment

Support for this work by the Office of Naval Research under Grant N00014-04-1-0303 is gratefully acknowledged.

References

[1]Hüttner, B., "Optical Properties of Polyvalent Metals in the Solid and Liquid State: Aluminum," *Journal of Physics: Condensed Matter*, Vol. 6, No. 13, 1994, pp. 2459–2474.

[2]Sobol, E. N., *Phase Transformations and Ablation in Laser-Treated Solids*, Wiley, Hoboken, NJ, 1995, pp. 12–15.

[3]Touloukian, Y. S., *Thermophysical Properties of High Temperature Solid Materials*, Vols. 2 and 3, IFI/Plenum, New York, 1967.

[4]Touloukian, Y. S., and DeWitt, D. P., "Thermal Radiative Properties; Metallic Elements and Alloys," *Thermophysical Properties of Matter*, edited by Y. S. Touloukian and C. Y. Ho, Vol. 7, The TPRC Data Series, IFI/Plenum, New York, 1970.

[5]Touloukian, Y. S., and Ho, C. Y., *Thermophysical Properties of Selected Aerospace Materials. Part I: Thermal Radiative Properties*, IFI/Plenum, New York, 1976.

[6]Dausinger, F., and Shen, J., "Energy Coupling Efficiency ion Laser Surface Treatment," *Iron and Steel Institute of Japan Journal*, Vol. 33, No. 9, 1993, pp. 925–933.

[7]Wieting, T. J., and Schriempf, J. T., "Infrared Absorptance of Partially Ordered Alloys at Elevated Temperatures," *Journal of Applied Physics*, Vol. 47, No. 9, 1976, pp. 4009–4011.

[8]Zhang, Z., and Modest, M. F., "Temperature-Dependent Absorptances of Ceramics for Nd:YAG and CO_2 Laser Processing Applications," *Journal of Heat Transfer*, Vol. 120, No. 2, 1998, pp. 322–327.

[9]Ordal, M. A., Long, L. L., Bell, R. J., Bell, S. E., Bell, R. R., Alexander, R. W., Jr., and Ward, C. A., "Optical Properties of the Metals Al, Co, Cu, Au, Fe, Pb, Ni, Pd, Pt, Ag, Ti, and W in the Infrared and Far Infrared," *Applied Optics*, Vol. 22, No. 7, 1983, pp. 1099–1119.

[10]Arnold, G. S., "Absorptivity of Several Metals at 10.6 μm: Empirical Expressions for the Temperature Dependence Computed from Drude Theory," *Applied Optics*, Vol. 23, No. 9, 1984, pp. 1434–1436.

[11]Xie, J., and Kar, A., "Laser Welding of Thin Sheet Steel with Surface Oxidation," *Welding Journal*, Vol. 78, No. 10, 1999, pp. 343–348.

[12]Chen, J., and Ge, X.-S., "An Improvement on the Prediction of Optical Constants and Radiative Properties by Introducing an Expression for the Damping Frequency in Drude Model," *International Journal of Thermophysics*, Vol. 21, No. 1, 2000, pp. 269–280.

[13]Giulietti, D., and Lucchesi, M., "Emissivity and Absorptivity Measurements on Some High-Purity Metals at Low Temperature," *Journal of Physics D: Applied Physics*, Vol. 14, No. 5, 1981, pp. 877–881.

[14]Sokolov, A. V., *Optical Properties of Metals*, Elsevier, New York, 1967, pp. 130, 131.

[15]Weaver, J. H., and Frederikse, H. P. R., "Optical Properties of Metals and Semiconductors," *CRC Handbook of Chemistry and Physics*, 77th ed., edited by D. R. Lide, CRC Press, Boca Raton, FL, 1996, pp. 12.126–12.150.

[16]Lide, D. R., "Electrical Resistivity of Pure Metals," *CRC Handbook of Chemistry and Physics*, 77th ed., edited by D. R. Lide, CRC Press, Boca Raton, FL, 1996, pp. 12.40, 12.41.

[17]Ashcroft, N. W., and Sturm, K., "Interband Absorption and the Optical Properties of Polyvalent Metals," *Physical Review B*, Vol. 3, No. 6, 1971, pp. 1898–1910.